Pressure–Voltage Trap for DNA near a Solid-State Nanopore

A Pressure-Voltage Trap for DNA near a Solid-State Nanopore

*David P. Hoogerheide†, Bo Lu†, and Jene A. Golovchenko†‡**

†Department of Physics, Harvard University, Cambridge, Massachusetts 02138, U

‡School of Engineering and Applied Sciences, Harvard University, Cambridge, Massachusetts 02138, USA

ABSTRACT: We report the formation of a tunable single DNA molecule trap near a solid-state nanopore in an electrolyte solution under conditions where an electric force and a pressure-induced viscous flow force on the molecule are nearly balanced. Trapped molecules can enter the pore multiple times before escaping the trap by passing through the pore or by diffusing away. Statistical analysis of many individually trapped molecules yields a detailed picture of the fluctuation phenomena involved, which are successfully modeled by a one-dimensional first passage approach.

KEYWORDS: Solid-state nanopores, pressure gradient, DNA single-molecule detection, DNA trapping, DNA translocation attempts

Passing DNA through electrolyte-filled solid-state[1, 2] and protein[3] nanopores under an applied voltage bias is now a well-established technique for single-molecule studies. This method is of particular interest for technologies such as strand sequencing of DNA[4-7] and characterization of other charged polymers such as proteins.[8, 9]

In DNA nanopore experiments, the voltage bias attracts DNA molecules to the electrolyte-filled nanopore and threads them through. The passage, or "translocation", of each DNA molecule is detected by the change in the ionic current through the nanopore while the molecule is in the pore. The voltage bias is thus responsible for the capture,[10, 11] threading,[12-14] and detection of DNA molecules. These multiple roles strongly constrain the range of voltage biases (and hence forces on the DNA molecule) available for experiments. Large voltage biases translocate DNA too quickly to be detected, while small voltage biases produce both a smaller electronic signal and a lower rate of capture. As a result, nanopore-based studies have been largely limited to the intermediate-voltage regime between 30 and 300 mV where most DNA translocation experiments are carried out.

In recent work,[15] we showed that the threading and detection functions could be decoupled by the addition of a pressure bias across a voltage-biased solid-state pore. In a pressure-voltage (P-V) biased pore, the net force (and hence the speed) of a DNA molecule could be reduced by an order of magnitude without a similar reduction in the ionic current through the nanopore. In this paper, we report a surprising discovery: when the net force around the pore is reduced nearly to zero, a trap for DNA forms just outside the boundary of the pore. While in this "P-V trap", individual DNA molecules attempt to translocate multiple times before successfully translocating or diffusing away. Tuning the trap enables a direct measurement of the statistics of DNA capture

and loss in nanopores. We also show that the fluctuation phenomena leading to DNA capture and loss can be understood in terms of a one-dimensional first-passage formulation.

The notion that the interplay of a barrier to translocation and long-range attractive forces in a voltage-biased nanopore might create a trap near the entrance of the pore has been proposed before to explain capture rate data in voltage-biased nanopores.[11, 16-20] The approach reported here is analogous, except the origin of the "barrier" to translocation is not entropic or steric, but rather depends on an experimentally adjustable balance of the applied pressure and voltage gradients.

RESULTS AND DISCUSSION

Figure 1a shows the experimental setup used for the formation of a P-V trap.[15] Note the convention that positive V and ΔP both induce DNA translocation through the pore, while negative values retard translocation. Thus, if positive ΔP and negative V are applied across the membrane, the directions of the forces on the molecule are as shown in Figure 1a. The behavior of DNA under these conditions, in which the DNA is captured from the high-pressure side of the membrane, can be anticipated *via* finite element calculations. Figure 1b shows the calculated net force on one Kuhn length of double-stranded DNA (dsDNA) near a nanopore. The distance is defined as the distance along the pore axis from the center of the nanopore to the center of the rod. The calculations show that at $\Delta P = 2.2$ atm and $V = -100$ mV, the net force on the molecule crosses zero as the molecule approaches the inside of the nanopore. At distances less than the zero crossing, the calculations predict that the electric field is dominant, and the molecule's motion is directed away from the pore. At distances greater than the zero crossing, the viscous effect of the pressure-induced flow field is dominant, and the molecule is attracted to the pore.

The net effect is that the molecule is focused towards the zero crossing point and trapped in its vicinity. The streaming potential is calculated to be 0.3 mV/atm and does not significantly affect the properties of the trap.

The existence of a force direction crossover near the nanopore can be understood as follows. Far from the pore, both the pressure-induced flow field and the electric field decay inversely with the square of the distance from the pore. Consider the case where the net force arising from the action of these fields on a molecule is zero, *i.e.* the forces are balanced. Near the nanopore, the pressure-induced flow field is suppressed by the no-slip boundary conditions at the walls of the pore, leading to a parabolic radial force profile inside the pore, as discussed previously.[15] The electric field is not subject to these boundary conditions and therefore dominates near the pore. If the pressure is then increased slightly, the electric field still dominates inside the pore, but the pressure-induced flow field dominates at large distances from the pore, leading to a force direction crossover near the pore.

We report on the results of two experiments in which such a P-V trap was formed. We first studied 615 bp dsDNA in a nanopore of conductance 59 nS, using ΔP at 11 values between 1.64 atm and 2.44 atm and $V = -100$ mV. The rms noise level (calculated by integrating the current noise power spectral density from 200 Hz to 40 kHz) was 12 pA at $V = -100$ mV. In a second experiment, we acquired similar data using 3.27 kbp dsDNA molecules in a nanopore of conductance 126 nS with $\Delta P = 0.865$ atm and $V = -100$ mV. The lower pressure is required because the diameter of the second pore is larger, and the pressure-derived force is proportional to the cross-sectional area of the pore.[15] The rms noise level in this experiment was 13.1 pA.

Representative events for 615 bp dsDNA at $\Delta P = 2.06$ atm and $V = -100$ mV are shown in Figure 1c-d. The event shown in Figure 1c is typical of translocation experiments: the event is

isolated and has a square shape with a single beginning and end. A second event shown in Figure 1d displayed an unusual time structure in that after an initial sharp current blockage of short duration, the ionic current temporarily returns to the open pore value before a blockade of similar duration. Other events are shown on an extended scale for 615 bp dsDNA at ΔP = 1.76 atm and V = –100 mV in Figure 1f. Corresponding data are shown for 3.27 kbp dsDNA with ΔP = 0.865 atm and V = –100 mV in Figure 1g. The events generated by longer molecules show additional unusual structure and especially wide current level fluctuations within each event. This case is discussed qualitatively in section S1 of the Supporting Information.

In the following discussion, we demonstrate that these observations can be understood by the simple picture represented in Figure 1e. Each "event" reflects the motion of a single molecule, as seen by comparing the short time scales of each event to the long time intervals between events. Individual excursions from the open pore current within each event represent the insertion of one end of the molecule into the pore in an "attempt" at translocation. A temporary return of the ionic current to its open pore level corresponds to a failed translocation attempt, in which the molecule is expelled backwards from the nanopore to its trapped position. Failed attempts are shown in red in Figures 1d-e. If the return to the open pore current is permanent, *i.e.* followed by no additional structure for an extended period such as the typical time between molecule captured (0.01~10sec), the attempt was successful or the molecule was lost from the trap by diffusion. Such attempts are shown in green in Figures 1c,e.

Inspection of the current traces shown in Figures 1f-g shows that the temporary returns to the open pore current are much shorter than the time interval between individual events. To quantify this observation, we have developed a threshold detection algorithm. The current trace is 5-sample median filtered and compared to a threshold of 50 pA above the average open pore

current and about 70% of full current blockage of DNA translocation. The times at which the filtered current trace crosses the threshold are recorded. Each of these "threshold crossings" is categorized as "rising" or "falling" based on whether the current is increasing or decreasing at the threshold crossing. Threshold crossings separated by less than 13 μs are indistinguishable from noise and are discarded. The time intervals Δt between rising threshold crossings are then computed, as shown in the inset to Figure 2a. These time intervals are compiled into the "interval histograms" shown in Figure 2a for 615 bp DNA for each pressure bias. A logarithmic scale is used for the histogram bins because the time intervals vary over orders of magnitude.

Each interval histogram is composed of two peaks, one at long intervals (0.1-10 s), and the other at short intervals (10^{-4}-10^{-3} s). The peaks can be easily separated with a cutoff that varies with pressure, ranging between 1 ms for the highest pressures to 15 ms for the lowest. This shows that some of the rising threshold crossings occur in well-defined clusters (already shown qualitatively in Figure 1). The long intervals correspond to the time elapsed between clusters, while the short intervals correspond to threshold crossings within clusters. The long intervals are Poisson distributed (shown as the heavy dashed line in Figure 2a), and we naturally interpret this peak to be the distribution of intervals between the captures of different DNA molecules.[21] Then each cluster represents the multiple probing of the pore by a single DNA molecule, and each rising threshold crossing within the cluster represents the beginning of a translocation "attempt", *i.e.* the insertion of the molecule end into the nanopore. If a cluster contains multiple rising threshold crossings, it is referred to as a "multiple-attempt" event. Events with only one rising threshold crossing are "single-attempt" events.

Figure 2b shows the event duration distributions for unfolded translocation events for 615 bp dsDNA at $\Delta P = 1.87$ atm and $V = -100$ mV. Two distributions are shown: the event duration

distributions of the single-attempt events and the last attempt of the multiple-attempt events. The two distributions are essentially indistinguishable, indicating that statistically the ultimate fate of molecules that produce single- and multiple-attempt events is the same. This interpretation is consistent with our inference that only the last attempt corresponds to translocation, and the prior attempts, *i.e.* the "all but last attempts", correspond to failed attempts of the same molecule.

Figure 2c shows the interval histogram for 3.27 kbp DNA for ΔP = 0.865 atm and V = –100 mV. The peak separation between attempts and captures occurs at about 50 ms (vertical dashed line). Figure 2d shows the distribution of last attempt durations. The average translocation time was 2.6 ms, a factor of 24 greater than the translocation time for this length of molecule in a standard translocation experiment at V = 100 mV.[15]

The same analysis can be applied to a control experiment with a nanopore biased with V = 100 mV and ΔP = 0 atm. No short-interval peak is observed in the interval histogram. As discussed in Supporting Information Section S3, the results of the control experiment suggest that the populations of very short events that are often observed with voltage-biased nanopores are not actually "collisions" of DNA molecules with the pore, as has been widely thought[22].

The existence of multiple-attempt events in a P-V biased nanopore raises the question of whether or not all molecules that attempt to go through the pore ultimately succeed. In Figure 3a-b, we plot the distribution $N_{last}(t)$ of the "last attempt" duration t (both "single-attempt" and "multiple-attempt" events) for 615 bp DNA at ΔP = 1.64, 1.70, and 1.76 atm. We also consider the distribution of the durations of the "all but last attempts", or $N_{abl}(t)$. On the same axes as $N_{last}(t)$, we plot a scaled distribution $P_{abl}(t) = N_{abl}(t)\int_0^{100\ \mu s} N_{last}(t')\,dt' \Big/ \int_0^{100\ \mu s} N_{abl}(t')\,dt'$, where the integrals denote discrete sums over the distributions. At ΔP = 1.64, $N_{last}(t)$ and $P_{abl}(t)$ are

essentially indistinguishable. As ΔP increases, a clear peak in $N_{last}(t)$ around 300 μs emerges that is not observed in $P_{abl}(t)$.

The upper panel of Figure 3c shows a schematic interpretation of these observations. If the duration of the last attempt is in the peak at 300 μs, it is likely to be a successful translocation attempt. The distribution of the durations of failed translocation attempts is indistinguishable from the distribution of the durations of failed attempts that occur before a successful translocation attempt. This accounts for the close correspondence in shape between $N_{last}(t)$ and $P_{abl}(t)$ at low pressures and for $t < 100\ \mu s$ for the three pressures shown. We assume such molecules are lost to diffusion or surface adhesion. The probability that a last attempt with duration t represents such a failed translocation is then given by $p_{fail}(t) = P_{abl}(t) / N_{last}(t)$, as shown in the lower panel of Figure 3c.

Figure 3d shows the same analysis applied to the 3.27 kbp DNA data. Here the separation at about 500 μs between the failed and successful translocations is very clear. For this experiment molecules that ultimately fail to translocate, *i.e.* are lost by diffusion, account for about 22% of the observed events, and they are excluded from the translocation time distribution shown in Figure 2d.

Figure 4a shows the fraction of events that fail to translocate for the 615 bp dsDNA at $V = -100$ mV over the full range of ΔP. This value is directly calculated from the histograms in Figure 3a-b as $\int_t P_{abl}(t)\,dt \Big/ \int_t N_{last}(t)\,dt$. Error bars are calculated with the bootstrap method[23]. At low ΔP the electrical force in the pore dominates, and all of the molecules eventually escape from the trap without translocating. At high ΔP viscous forces dominate, and the molecules translocate through the pore directly or stay in the trap until they translocate.

The average interval between the first and last observation of the molecule in the pore, or the average trapped time of successful translocation events, is shown in Figure 4b as a function of ΔP. From high to low ΔP the average trapped time increases by over an order of magnitude. Because of the significant overlap between $N_{last}(t)$ and $P_{abl}(t)$, we use the probability of failed translocation $p_{fail}(t)$ (see Figure 3c) to select the successful events in a statistical fashion. For each event with last attempt duration t, the event is deemed successful if a randomly chosen number between 0 and 1 is greater than $p_{fail}(t)$. This procedure is combined with the bootstrap method to calculate the average trapped time for successful events, as shown in Figure 4b.

We now show that the loss rate and trapping time can be understood in the context of a one-dimensional first passage approach. We model the 615 bp dsDNA in the P-V trap as a point particle diffusing in a force field that depends on ΔP and V. The pressure-derived forces F_p and voltage-derived forces F_V are not strongly coupled, allowing the net force to be written as $F(x) = \alpha F_p(x) + \beta F_V(x) - k_B T / x$. The force fields are calculated by finite-element methods[24] using a 200-nm long rod coaxial to the nanopore to model 615 bp dsDNA. The distance x from the nanopore is defined such that $x = 0$ is the position where the front of the DNA molecule is in the center of the nanopore. The coefficients α and β are parameters that compensate for uncertainties in the geometry of the nanopore, the surface charge of the DNA and the nanopore, and the assumption that the molecule is coaxial with the pore. For example, we expect $\alpha \lesssim 0.5$ because the average flow rate through a cylindrical pipe is about half that of the maximum. The final term in the expression for $F(x)$ is an entropic force that arises from the collapse of three-dimensional diffusion outside the pore to one-dimensional diffusion[10]. This term is only included when the molecule is outside the nanopore and is suppressed for $x < 0$.

We turn to a one-dimensional first-passage approach developed previously to describe the escape of dsDNA molecules from a diffusive trap[25]. We define the distributions of escape times $f_s(x,t)\,dt$ and $f_l(x,t)\,dt$ that represent the probabilities, respectively, that the DNA passes through the pore successfully or is lost to diffusion within a time between *t* and *t* + *dt* given a starting position *x*. These probability functions obey an equation adjoint to the 1-D Smoluchowski equation:

$$\frac{\partial f_{s,l}(x,t)}{\partial t} = \frac{F(x)}{\gamma}\frac{\partial f_{s,l}(x,t)}{\partial x} + D\frac{\partial^2 f_{s,l}(x,t)}{\partial x^2}$$

with boundary conditions $f_s(-L,t) = \delta(t)$; $f_s(x_{esc},t) = 0$; $f_l(-L,t) = 0$; $f_l(x_{esc},t) = \delta(t)$, and initial values $f_s(x,0) = 0\ (x > -L)$; $f_l(x,0) = 0\ (x < x_{esc})$. Here *D* and γ are the diffusion constant and drag coefficient, which are related through the fluctuation-dissipation theorem and are taken to be independent of position. L is the length of the DNA molecule, while x_{esc} is the position of the boundary at which the molecule is considered to be lost. The average trapped time of a successful translocation is given by $\tau_s(\Delta x) = \int_0^{+\infty} t f_s(\Delta x,t)\,dt$, while the fraction of lost events is $\pi_l(\Delta x) = \int_0^{+\infty} f_l(\Delta x,t)\,dt$, where Δx represents the offset in the initial position of the molecule from the condition where the front of the molecule is in the center of the nanopore. Because we expect to observe full current blockage only when the molecule is inserted completely into the nanopore, this parameter is closely related to the pore length.

The first passage model is optimized using non-linear least squares regression with five free parameters: α, β, *D*, Δx, and x_{esc}. The optimized model prediction for π_l and τ_s are shown as the solid curves in Figure 4a-b along with the values obtained from the 615 bp data . The fit is quite good. The parameter values are $\alpha = 0.382 \pm 0.003$, $\beta = 0.261 \pm 0.002$,

$D = 10.6 \pm 0.5\ \mu\text{m}^2\ \text{s}^{-1}$, $\Delta x = -24 \pm 6$ nm, and $x_{esc} = 445 \pm 26$ nm. These are reasonable values; the diffusion constant in particular is in excellent agreement with the measurements of DNA diffusion under very small forces in nanopores[25]. The small value of β suggests that the surface charge of the pore is large, about -120 mC/m^2.[24, 26, 27] The escape radius corresponds to a center-of-mass position from the membrane of about 500 nm, which is half the average separation of 615 bp dsDNA molecules at the concentrations used in this experiment. It is therefore not surprising that this is the distance at which we cannot distinguish between molecules which have diffused away and other molecules which are newly captured in the P-V trap.

The success of this model in describing the observed trapping dynamics can be attributed in part to the choice of short 615 bp dsDNA for the experiments, for three reasons. First, the molecule can be approximated by a point particle at relatively short distances from the pore. Second, the center of mass diffusion constant (relevant outside the pore)[28] and the diffusion constant of the molecule inside the pore[26] are approximately equal. Finally, the entropic cost to confine the molecule in the pore is minimal. For longer molecules, it is much more difficult to write down the relevant force field. The transition from a three-dimensional center-of-mass picture to a one-dimensional length-wise diffusion picture takes place over a larger region outside the nanopore. Entropy, which figures prominently in models of the capture rate in voltage-biased nanopores[16-18], is likely to provide an additional barrier to insertion of the molecule in the pore. Finally, a position-dependent diffusion constant must be employed to further differentiate between center-of-mass and length-wise diffusion. Despite these modeling challenges, we expect the methods developed in this work to be an important probe of the roles of geometry and entropy in the capture of polymers into nanopores[29-31].

CONCLUSION

We have shown that with the right combination of applied voltage and pressure gradients it is possible create a single DNA molecule trap at the entrance to a solid-state nanopore. The lifetime of a molecule remaining in the trap has been controlled with the external pressure and is well described by a first passage approach to a drift-diffusion model. This P-V trap enables the slowing of molecule translocation to the point where the fluctuating motion of a single DNA molecule can be measured and studied. We anticipate that this new capability will enhance the utility of nanopore detectors and provide new insights and understanding into single polymer dynamics in confined spaces.

METHODS

A free-standing low-stress silicon nitride membrane separated two reservoirs of electrolyte (1.6 M KCl buffered at pH 8 by 10 mM tris buffer and was stabilized against multivalent ions by 1 mM EDTA) in a flow cell. The membrane contained a single nanopore of diameter ~ 10 nm created by a focused electron beam.[2] One side of the flow cell was maintained at atmospheric pressure. DNA molecules were injected into the other reservoir at concentrations of 2 ng/μl. This reservoir was then brought to a pressure ΔP above atmospheric pressure with a regulated nitrogen tank. A voltage bias V was applied across the membrane using Ag/AgCl electrodes in the two reservoirs, and the resulting ionic current was monitored using an Axopatch 200B current amplifier (Molecular Devices, Sunnydale, CA). The electrode on the high-pressure side was grounded. Electrical signals were hardware filtered with a 40 kHz 8-pole low-pass Bessel filter before digitization at 250 kHz.

Finite element calculations were performed using COMSOL 4.3 software (COMSOL, Inc., Burlington, MA) based on a Poisson-Boltzmann-Navier-Stokes formalism previously described.[25] The calculations predict both electronic and viscous forces on the molecule, including forces arising from electrokinetic phenomena such as electroosmosis and streaming currents.[28] The DNA was modeled as a 100-nm long rigid cylindrical rod (radius 1.1 nm) concentric with the nanopore and held stationary at varying distances from the nanopore. The nanopore was modeled as a hole of radius 5 nm in a 20-nm thick membrane.

DNA molecules were prepared as previously reported.[15]

Conflict of interest: The authors declare no competing financial interest.

Acknowledgment. We thank Z. Tang for helpful assistance. This work was supported by National Institutes of Health Award No. HG003703 to J. Golovchenko and D. Branton.

Supporting Information Available: A brief discussion of transient deep blockages, event duration/current blockage histograms for the 615-bp dsDNA data, a discussion of translocation attempts in voltage-only experiments, a discussion of the optimized force profiles, and the capture rate and average translocation speed. This material is available free of charge *via* the Internet at http://pubs.acs.org.

FIGURES

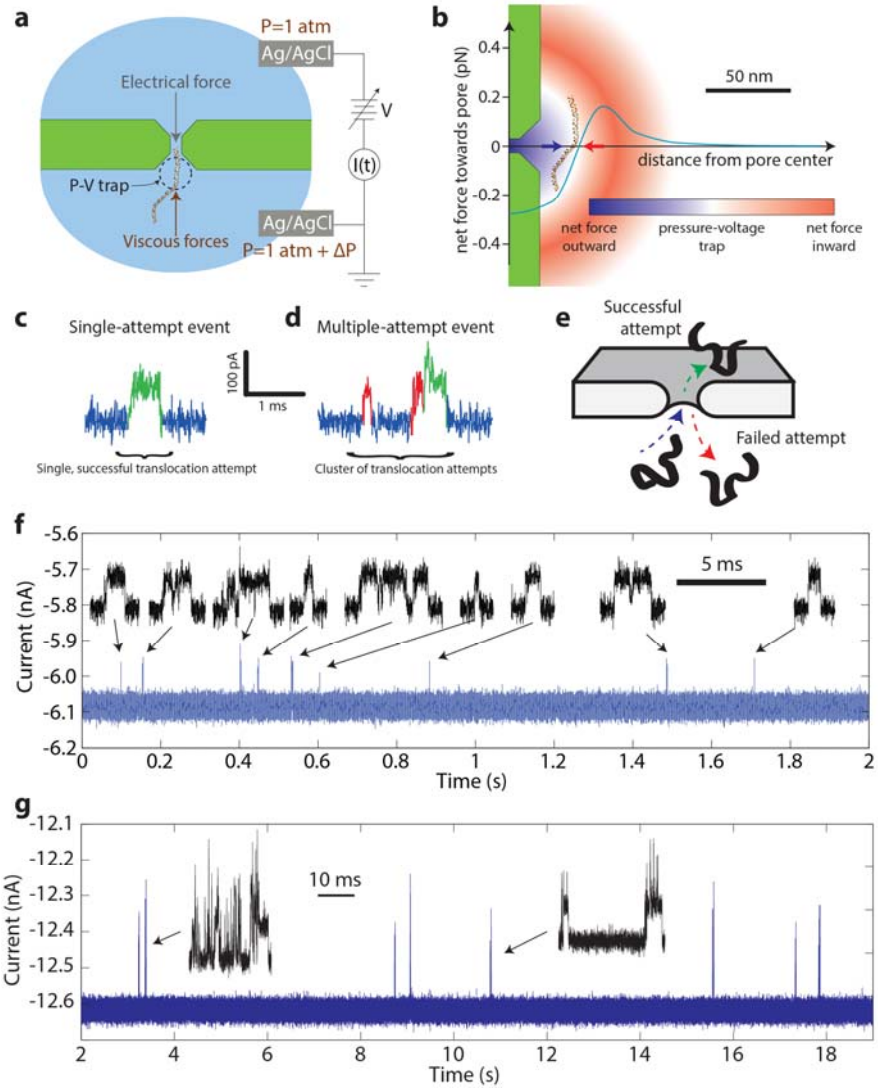

Figure 1. (a) Schematic of DNA translocation experiment with variable voltage and pressure. (b) Finite element calculation of the net force on 100 nm long dsDNA on the axis of the pore using $V = -100$ mV and $\Delta P = 2.2$ atm. Positive forces are directed toward the pore; negative forces are directed away from the pore. Arrows show how the DNA is focused toward the point of zero force. Color shading is a guide to the eye. (c-e) Events for 615 bp dsDNA molecules at $\Delta P = 2.06$ atm and $V = -100$ mV showing the difference between a single- (c) and multiple-attempt (d) event, and (e) a schematic representation of successful (green arrow and traces) and

failed (red arrow and traces) translocation attempts. (f) Data for 615 bp dsDNA molecules at ΔP = 1.76 atm and V = –100 mV showing a mixture of single- and multiple-attempt events. (g) Data for 3.27 kbp dsDNA molecules at ΔP = 0.865 atm and V = –100 mV showing extremely complex structures.

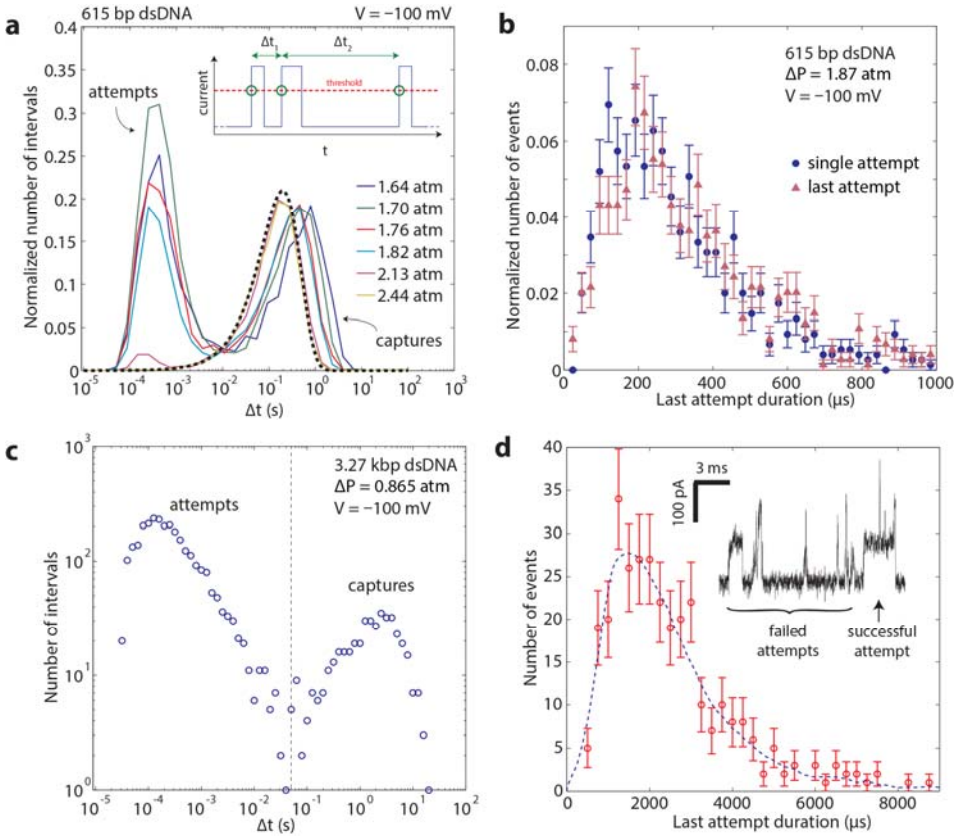

Figure 2. Interval and event duration histograms. (a) Interval histogram for 615 bp DNA at various pressures. The peak at longer times is the distribution of times between events (captures). The heavy dashed line shows a normalized theoretical Poisson distribution. All experiment distributions have been normalized to the number of events in the peak at longer times. The peak at shorter times is the distribution of time interval between attempts within a single event. Inset: pictorial representation of the threshold crossing algorithm used to generate the interval histogram. (b) Comparison of the event duration histogram of single-attempt events and the last attempt of multiple-attempt events for ΔP = 1.87 atm. (c) Interval histogram demonstrating the distinct time intervals characterizing captures and attempts for 3.27 kbp DNA. (d) Long event duration histograms for 3.27 kbp DNA. Inset: a typical long event. Failed attempts (see text) have been excluded when calculating the event duration histogram.

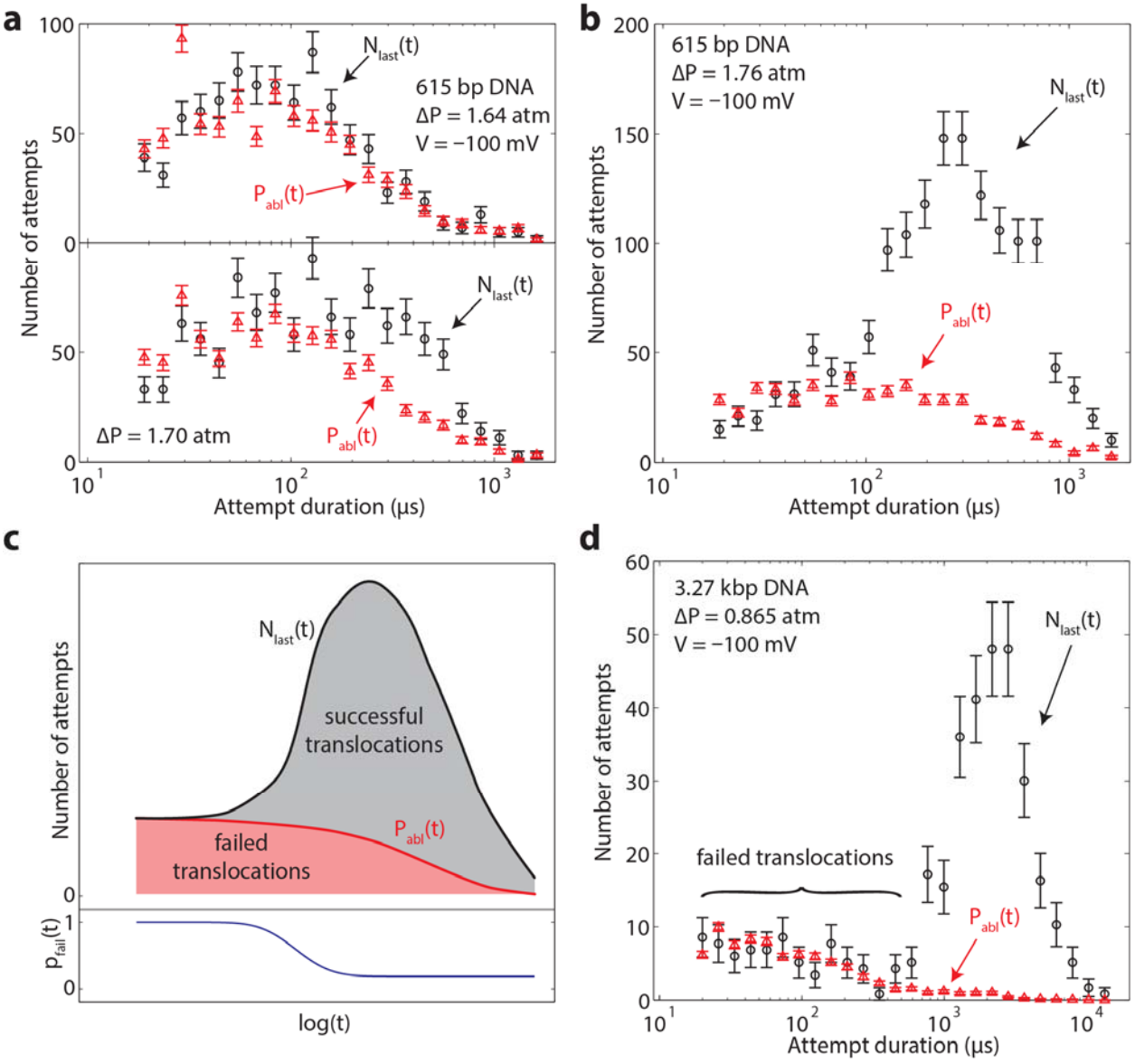

Figure 3. Analysis of failed translocations. (a-b) Logarithmic event duration histogram for 615 bp DNA at ΔP = 1.64, 1.70, and 1.76 atm. (c) Upper panel is the schematic interpretations of the event duration histograms. Lower panel is the calculation of $p_{fail}(t)$ used in the calculation of average trapped time of successful events. (d) Logarithmic event duration histogram for 3.27 kbp

DNA showing a clear separation between successful and failed translocations. In all panels $P_{abl}(t)$ has been scaled as described in the text.

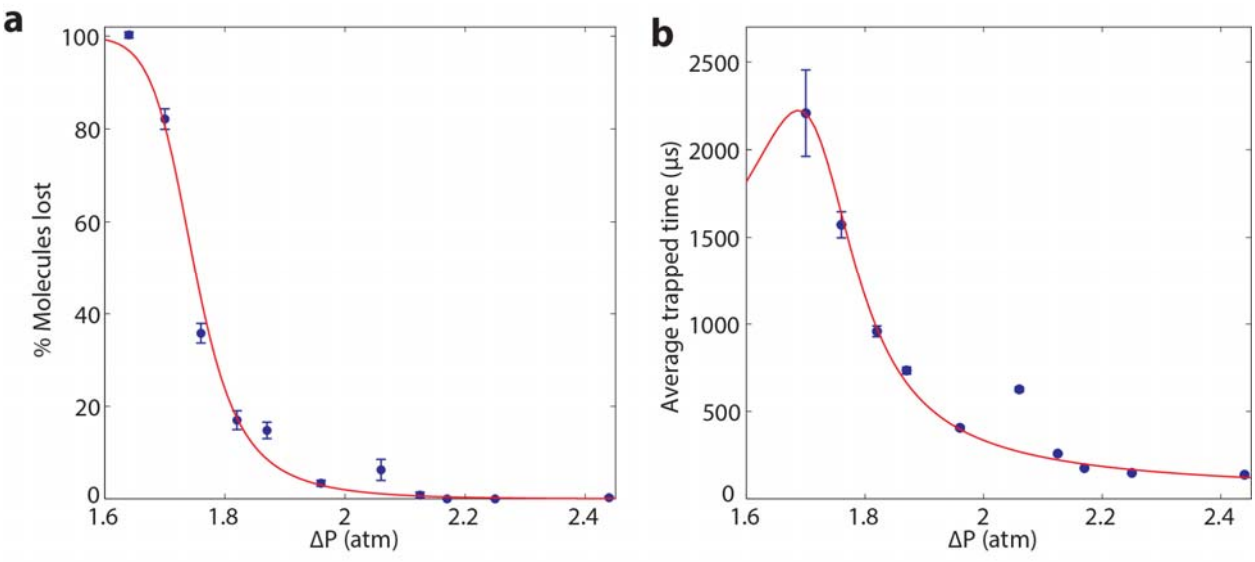

Figure 4. (a) Percentage of unsuccessful translocations at different pressures. The solid line is the prediction of the model in the text. (b) Average escape time of molecules in the P-V trap, for successful translocations only. The solid line is the prediction of the model in the text.

Corresponding Author

*Corresponding author: golovchenko@physics.harvard.edu.

REFERENCES

1. Li, J.; Stein, D.; McMullan, C.; Branton, D.; Aziz, M. J.; Golovchenko, J. A. Ion-Beam Sculpting at Nanometre Length Scales. *Nature* **2001**, *412*, 166-169.

2. Storm, A. J.; Chen, J. H.; Ling, X. S.; Zandbergen, H. W.; Dekker, C. Fabrication of Solid-State Nanopores with Single-Nanometre Precision. *Nat. Mater.* **2003**, *2*, 537-540.

3. Kasianowicz, J. J.; Brandin, E.; Branton, D.; Deamer, D. W. Characterization of Individual Polynucleotide Molecules Using a Membrane Channel. *Proc. Natl. Acad. Sci. U.S.A.* **1996**, *93*, 13770-13773.

4. Branton, D.; Deamer, D. W.; Marziali, A.; Bayley, H.; Benner, S. A.; Butler, T.; Di Ventra, M.; Garaj, S.; Hibbs, A.; Huang, X. H.; *et al.* The Potential and Challenges of Nanopore Sequencing. *Nat. Biotechnol.* **2008**, *26*, 1146-1153.

5. Derrington, I. M.; Butler, T. Z.; Collins, M. D.; Manrao, E.; Pavlenok, M.; Niederweis, M.; Gundlach, J. H. Nanopore DNA Sequencing with MspA. *Proc. Natl. Acad. Sci. U.S.A.* **2010**, *107*, 16060-16065.

6. Cherf, G. M.; Lieberman, K. R.; Rashid, H.; Lam, C. E.; Karplus, K.; Akeson, M. Automated Forward and Reverse Ratcheting of DNA in a Nanopore at 5-A Precision. *Nat. Biotechnol.* **2012**, *30*, 344-348.

7. Manrao, E. A.; Derrington, I. M.; Laszlo, A. H.; Langford, K. W.; Hopper, M. K.; Gillgren, N.; Pavlenok, M.; Niederweis, M.; Gundlach, J. H. Reading DNA at Single-Nucleotide Resolution with a Mutant MspA Nanopore and phi29 DNA Polymerase. *Nat. Biotechnol.* **2012**, *30*, 349-353.

8. Talaga, D. S.; Li, J. Single-Molecule Protein Unfolding in Solid State Nanopores. *J. Am. Chem. Soc.* **2009**, *131,* 9287-9297.

9. Han, A.; Creus, M.; Schurmann, G.; Linder, V.; Ward, T. R.; de Rooij, N. F.; Staufer, U. Label-Free Detection of Single Protein Molecules and Protein-Protein Interactions Using Synthetic Nanopores. *Anal Chem.* **2008**, *80*, 4651-4658.

10. Gershow, M.; Golovchenko, J. Recapturing and Trapping Single Molecules with a Solid-State Nanopore. *Nat. Nanotechnol.* **2007**, *2*, 775-779.

11. Wanunu, M.; Morrison, W.; Rabin, Y.; Grosberg, A. Y.; Meller, A. Electrostatic Focusing of Unlabelled DNA into Nanoscale Pores Using a Salt Gradient. *Nat. Nanotechnol.* **2010**, *5*, 160-165.

12. Storm, A. J.; Storm, C.; Chen, J.; Zandbergen, H.; Joanny, J.-F.; Dekker, C. Fast DNA Translocation through a Solid-State Nanopore. *Nano Lett.* **2005**, *5*, 1193-1197.

13. Lu, B.; Albertorio, F.; Hoogerheide, D. P.; Golovchenko, J. A. Origins and Consequences of Velocity Fluctuations during DNA Passage through a Nanopore. *Biophys. J.* **2011**, *101*, 70-79.

14. Mihovilovic, M.; Hagerty, N.; Stein, D. Statistics of DNA Capture by a Solid-State Nanopore. *Phys. Rev. Lett.* **2013**, *110*, 028102.

15. Lu, B.; Hoogerheide, D. P.; Zhao, Q.; Zhang, H.; Tang, Z.; Yu, D.; Golovchenko, J. A. Pressure-Controlled Motion of Single Polymers through Solid-State Nanopores. *Nano Lett.* **2013**, *13*, 3048-3052.

16. Grosberg, A. Y.; Rabin, Y. DNA Capture into a Nanopore: Interplay of Diffusion and Electrohydrodynamics. *J Chem. Phys.* **2010**, *133*, 165102.

17. Muthukumar, M. Theory of Capture Rate in Polymer Translocation. *J Chem. Phys.* **2010**, *132*, 195101.

18. Rowghanian, P.; Grosberg, A. Y. Electrophoretic Capture of a DNA Chain into a Nanopore. *Phys. Rev. E* **2013**, *87*, 042722.

19. Meller, A.; Nivon, L.; Branton, D. Voltage-Driven DNA Translocations through a Nanopore. *Phys. Rev. Lett.* **2001**, 86, 3435-3438.

20. Kowalczyk, S. W.; Kapinos, L.; Blosser, T. R.; Magalhães, T.; van Nies, P.; Lim, R. Y.; Dekker, C. Single-Molecule Transport across an Individual Biomimetic Nuclear Pore Complex. *Nat. Nanotechnol.* **2011**, *6*, 433-438.

21. Meller, A. Dynamics of polynucleotide transport through nanometre-scale pores. *J. Phys-Condens. Mat* **2003**, *15*, R581-R607.

22. Wanunu, M.; Sutin, J.; McNally, B.; Chow, A.; Meller, A. DNA Translocation Governed by Interactions with Solid-State Nanopores. *Biophys. J.* **2008**, *95*, 4716-4725.

23. Press, W. H. *Numerical Recipes 3rd edition: The Art of Scientific Computing*. Cambridge University Press: New York, NY, 2007.

24. Lu, B.; Hoogerheide, D. P.; Zhao, Q.; Yu, D. P. Effective Driving Force Applied on DNA inside a Solid-State Nanopore. *Phys. Rev. E* **2012**, *86*, 011921.

25. Hoogerheide, D. P.; Albertorio, F.; Golovchenko, J. A. Escape of DNA from a Weakly Biased Thin Nanopore: Experimental Evidence for a Universal Diffusive Behavior. *Phys. Rev. Lett.* **2013**, *111*, 248301.

26. Hoogerheide, D. P.; Garaj, S.; Golovchenko, J. A. Probing Surface Charge Fluctuations with Solid-State Nanopores. *Phys. Rev. Lett.* **2009**, *102*, 256804.

27. van der Heyden, F. H.; Stein, D.; Dekker, C. Streaming Currents in a Single Nanofluidic Channel. *Phys. Rev. Lett.* **2005**, *95*, 116104.

28. Nkodo, A. E.; Garnier, J. M.; Tinland, B.; Ren, H.; Desruisseaux, C.; McCormick, L. C.; Drouin, G.; Slater, G. W. Diffusion Coefficient of DNA Molecules during Free Solution Electrophoresis. *Electrophoresis* **2001**, *22*, 2424-2432.

29. Butler, T. Z.; Gundlach, J. H.; Troll, M. A. Determination of RNA Orientation during Translocation through a Biological Nanopore. *Biophys. J.* **2006**, *90*, 190-199.

30. Ying, Y.-L.; Li, D.-W.; Li, Y.; Lee, J. S.; Long, Y.-T. Enhanced Translocation of poly (dt) 45 through an α-hemolysin Nanopore by Binding with Antibody. *Chem. Commun.* **2011**, *47*, 5690-5692.

31. Wong, C. T. A.; Muthukumar, M. Polymer Translocation through α-hemolysin Pore with Tunable Polymer-Pore Electrostatic Interaction. *J. Chem. Phys.* **2010**, *133*, 045101.

Supporting Information

A Pressure-Voltage Trap for DNA near a Solid-State Nanopore

*David P. Hoogerheide†, Bo Lu†, and Jene A. Golovchenko†‡**

†Department of Physics, Harvard University, Cambridge, Massachusetts 02138, USA

‡School of Engineering and Applied Sciences, Harvard University, Cambridge, Massachusetts 02138, USA

S1. Transient deep blockages

In Figure 1f-g, inspection of individual long translocation attempts reveals that the current blockage occasionally increases for a short period of time from the level expected for a single strand. These "transient deep blockages" are typically observed in traditional translocation experiments at the beginning of an event, where they signal that the molecule was captured in the middle instead of at an end, and very occasionally at the end, indicating that the trailing end of the molecule was captured into the nanopore before the rest of the molecule completed the translocation process. When translocation is slowed by well-balanced forces, we observe an

increase in the number of transient deep blockages in the middle of translocation attempts (see Figure 1 of the main text).

We seek an explanation for transient deep blockages that is consistent with the data in the main text and Supporting Information. In Figure 1b of the main text, we have shown that the pressure force is dominant in the access region close to the nanopore, even when the forces on the molecule in the pore are balanced. Figure 1b of Ref. 6 also shows that in this balanced case the voltage-derived forces are dominant at the periphery of the pore. We therefore propose that in the case of slow translocation and relatively long molecules, the part of the molecule in the pore is moving sufficiently slowly that the trailing end has time to be driven into the pore by the pressure-driven flow, increasing the current blockage. We attribute the transience of the signal to the rapid ejection of this end by the voltage-derived forces at the periphery of the pore. When the forces are carefully balanced, there is not enough space for both the main strand and the trailing end in the region of the pore where the pressure force dominates (see Figure 1b of Ref. 15).

S2. Additional data for reduced-force 615 bp dsDNA experiments

Figure S1 documents the single- and multiple-attempt translocation events at each pressure using a two-dimensional current blockage-event duration histogram. For multiple-attempt events, the event duration and current blockage are determined only from the last attempt. The total number of events for each histogram is indicated. The distributions for the two types of events are indistinguishable (see also the inset to Figure 2b).

	Single-attempt events	Multiple-attempt events
1.64 atm	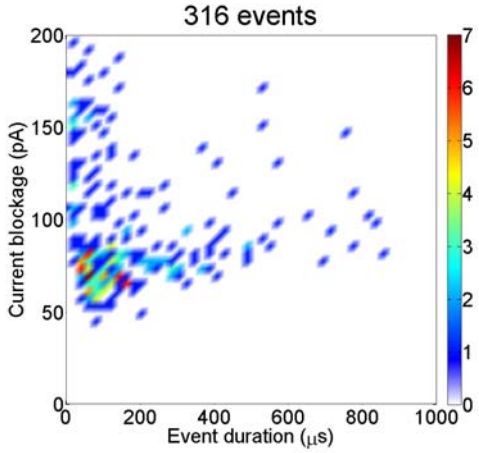	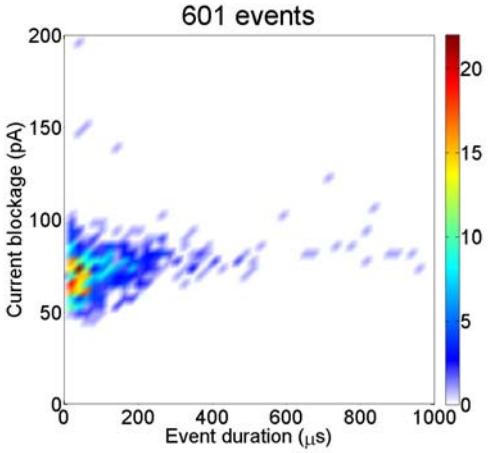
1.70 atm	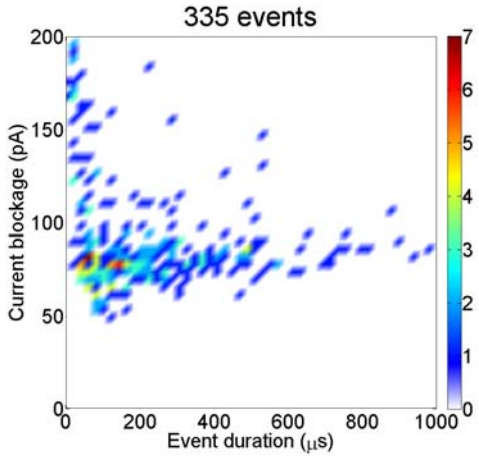	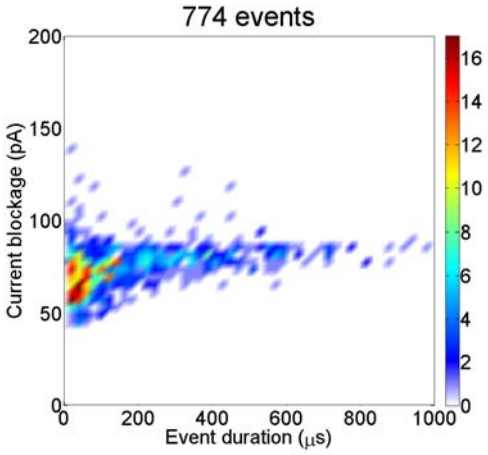
1.76 atm	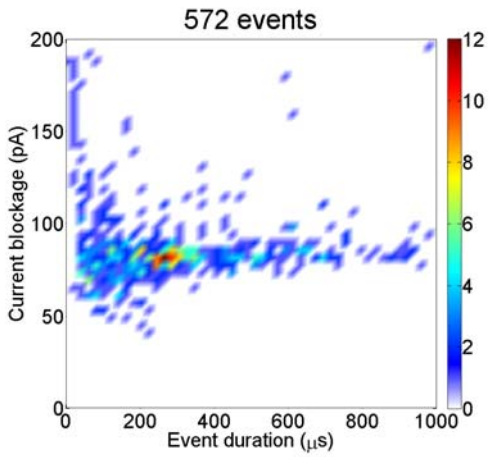	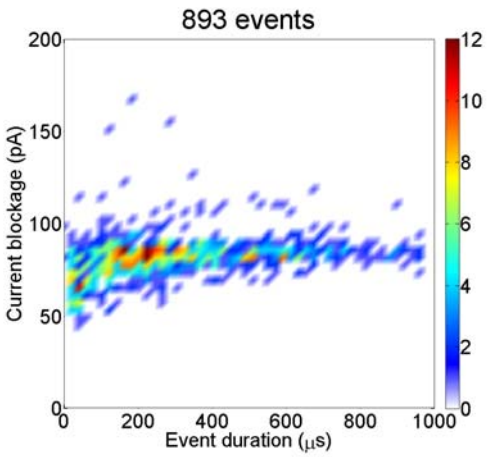

	Single-attempt events	Multiple-attempt events
1.82 atm	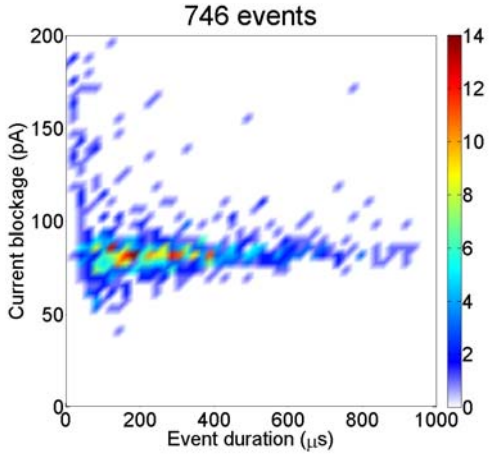	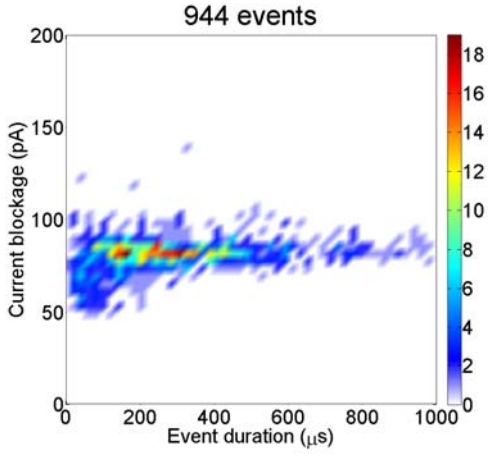
1.87 atm	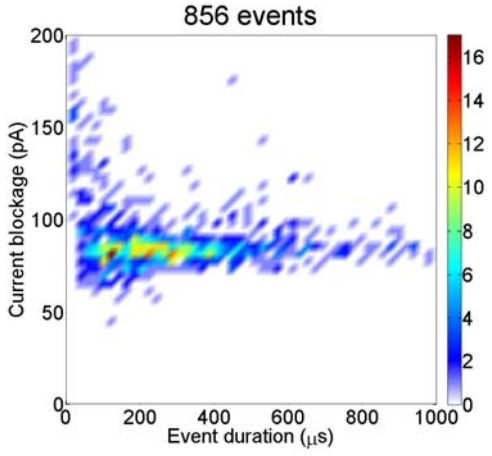	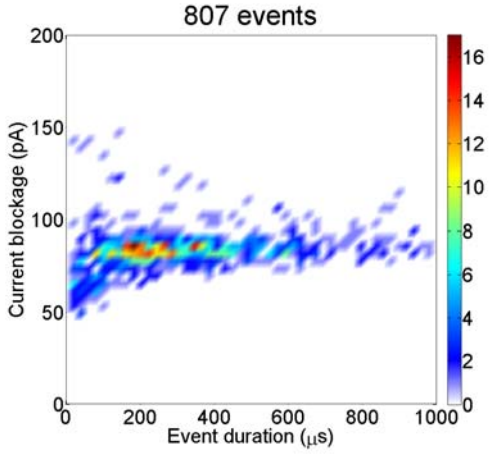
1.96 atm	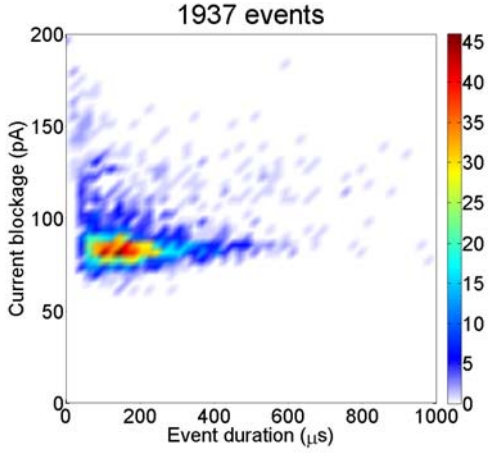	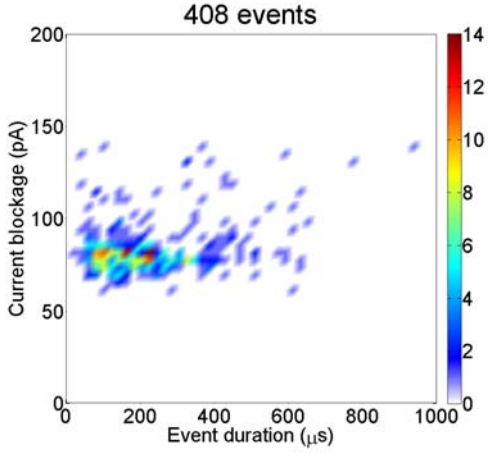

	Single-attempt events	Multiple-attempt events
2.06 atm	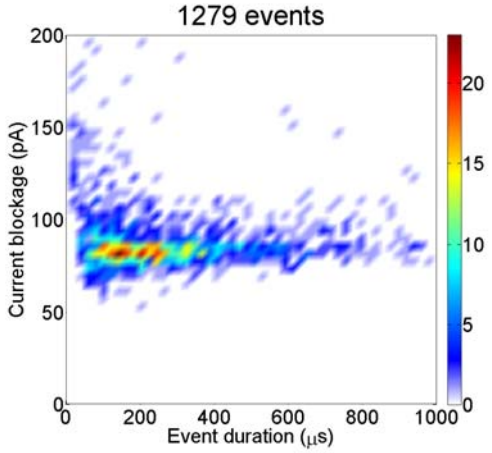	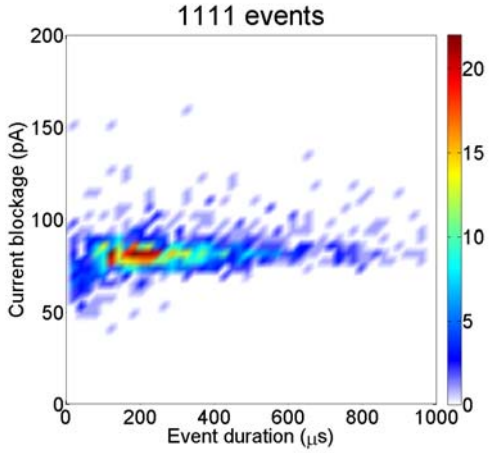
2.12 atm	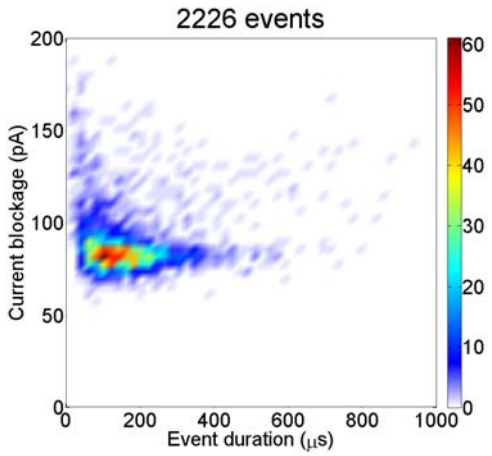	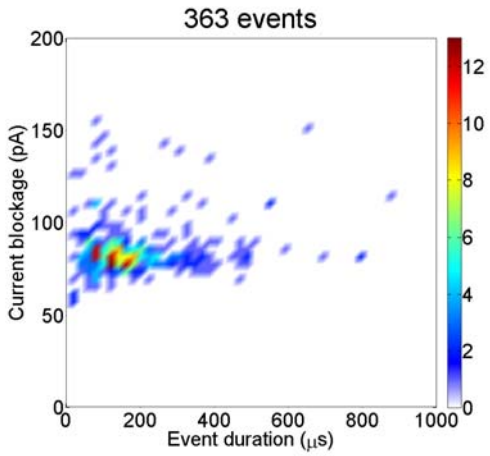
2.17 atm	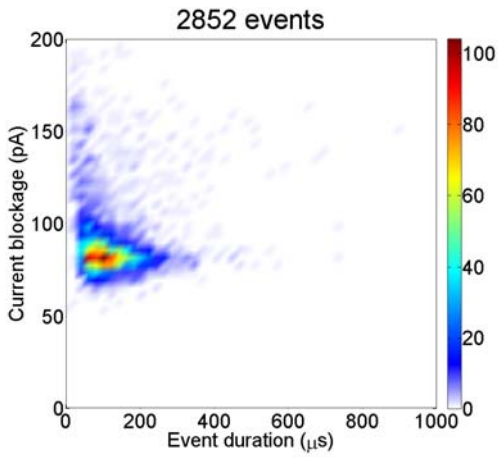	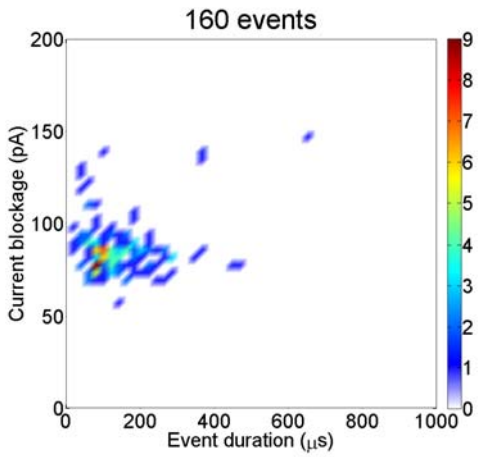

	Single-attempt events	Multiple-attempt events
2.25 atm	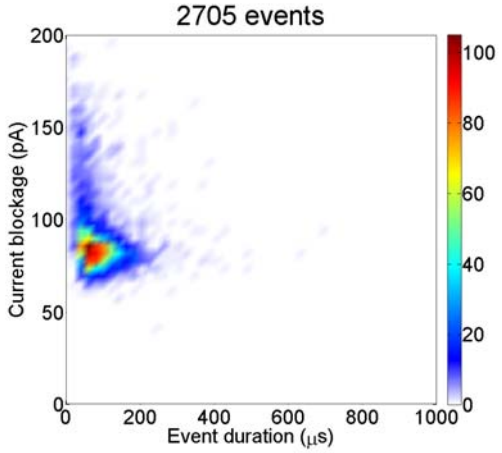	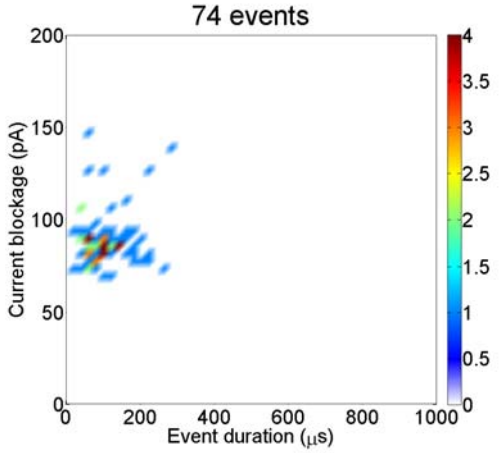
2.44 atm	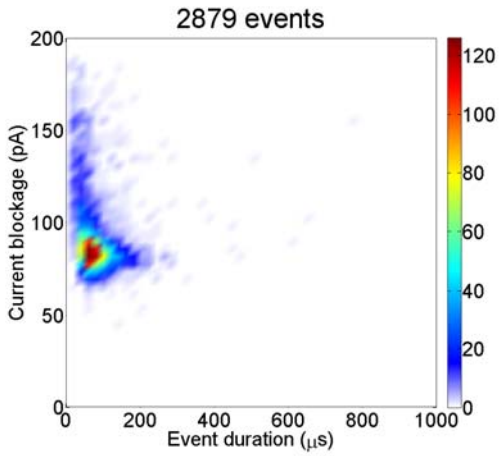	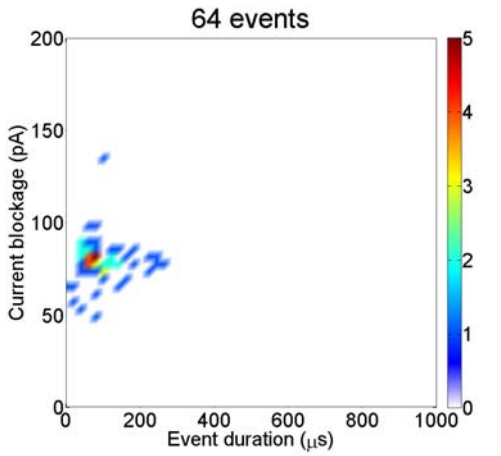

Figure S1. Density histograms of single-attempt and multiple-attempt events for 615 bp dsDNA at different pressures and –100 mV counter voltage.

S3. Translocation attempts in voltage-only experiments

In conventional translocation experiments involving only a voltage bias, very short events have routinely been detected and are distinguished from ordinary translocation events. Figure S2a,b shows data from a voltage-biased pore of diameter ~10 nm using V = +100 mV and 3.27 kbp dsDNA. The short events, marked in red, are clearly visible. These events have naturally been interpreted as translocation attempts or failed translocations.

The threshold detection algorithm can be applied to these data as well. The time interval histogram is shown in Figure 2c. As expected from extrapolation of the results of this study to the high-force regime, there is no high-frequency (short-time) peak in the time interval histogram. This demonstrates that there is no correlation between these short events and the next event. Thus these short events are not translocation "attempts" as described in this paper.

Could these events be molecules that fail to translocate and are then lost to diffusion? We assume that the dynamics of the 3.27 kbp dsDNA and 615 bp dsDNA are not significantly different, allowing us to estimate the expected loss rate for the 3.27 kbp dsDNA at V = 100 mV from the 615 bp dsDNA data. For the 615 bp dsDNA, a 22% loss rate occurs with ΔP = 1.82 atm and V = -100 mV, and the loss rate drops to < 1% at ΔP = 2.44 atm and V = -100 mV (see Figure 4a). This suppression of the loss rate is accompanied by an increase in the translocation speed of the 615 bp dsDNA by only a factor of 2 (Figure S3b). For 3.27 kbp dsDNA at ΔP = 0.865 atm and V = -100 mV, the loss rate is also about 20%. At ΔP = 0 atm and V = +100 mV, however, the translocation speed of 3.27 kbp dsDNA is a factor of 20 larger, so by analogy to the 615 bp dsDNA (where the suppression of the loss rate from 20% to <1% occurs with an increase in the translocation speed by a factor of 2) we expect the loss rate to be much less than 1%. The

observed fraction of spikes, however, is 11% for the 3.27 kbp dsDNA under V = +100 mV only, which is much too large to attribute all of them to molecules lost to diffusion.

We conclude that most of these short events are not collisions at all. They are likely due to some other phenomenon, such as the translocation of short DNA fragments, translocation of small impurities, or electronic noise.

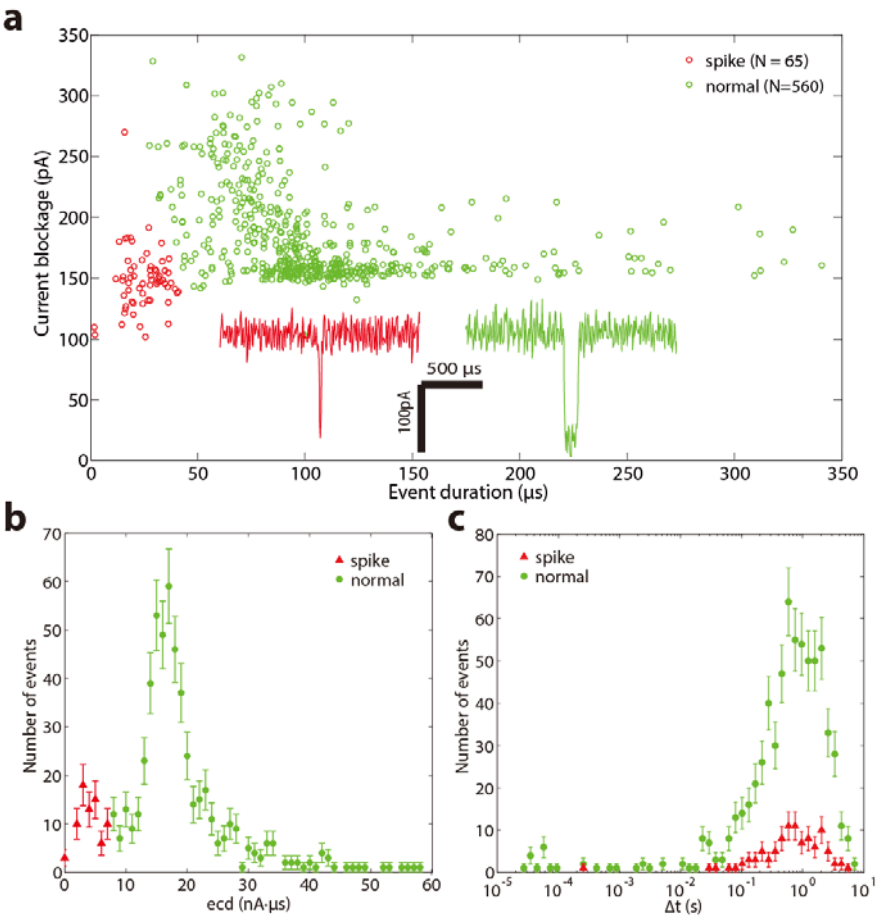

Figure S2. (a) Two dimensional current blockage/event duration histogram of ordinary translocation events (green) and very short events (red) in a conventional voltage-biased nanopore. (Inset) Typical events of each type. (b) Event charge deficit (ecd) histogram. (c) Time interval histogram showing the absence of a peak at short times. Also note that the time intervals

between the spikes and the next events are indistinguishable from the time intervals between normal events, showing that there is no correlation between spikes and normal events.

S4. Detailed results of finite element calculation

In Figure 4, we show the predictions of our optimized drift-diffusion model. The inset to Figure S3a shows the geometry of the calculation at $x = 0$, where the head of molecule is in the center of the nanopore. The main Figure S3a shows the force fields calculated using the optimized parameters for several pressures. Note that a true P-V trap, in which the force field crosses zero with a positive slope, exists only for some of the pressures, such as 1.76 atm and 1.70 atm, corresponding to those pressures at which the failure rate is about 50% and the dwell time is maximum. Multiple attempts at translocation are observed for the entire pressure range, however, because diffusive motion is significant relative to the force-induced motion for all the pressures studied here.

The curves in Figure S3a also help explain the experimental observation that the capture rate does not drop to zero at the same pressure as the average translocation speed, as shown in Figure S3b. This is consistent with the presence of a small attractive region near $x = 0$ and suggests that the attractive viscous forces are stronger than the repulsive electrical forces outside the nanopore. Note that the method for calculating the average translocation speed (which is meaningful only for successful translocations) is the same as the method used to calculate the average trapping time, as described in the text.

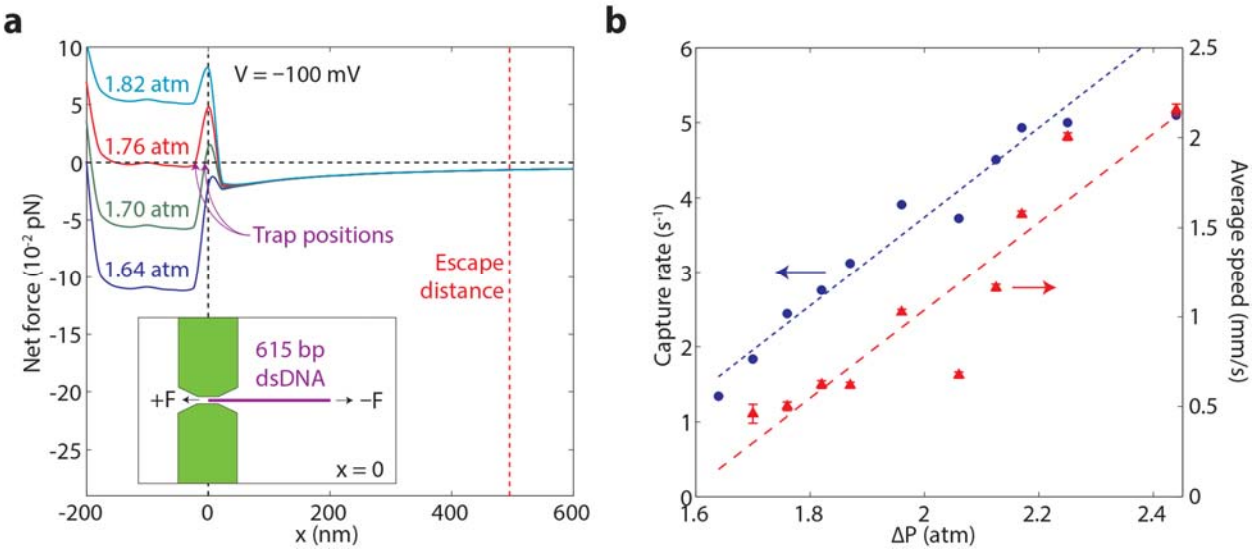

Figure S3. (a) Sample force fields used to calculate the curves in Figure 4a-b. Inset: geometry of the calculation at $x = 0$. (b) Comparison of the capture rate (left axis) and average translocation speed (right axis) at different pressures. Lines are regression fits to the data below $\Delta P = 2.3$ atm.